May 2007

Two-Port Stacked Piezoelectric Aluminum Nitride Contour-Mode Resonant MEMS

Gianluca Piazza
University of Pennsylvania, piazza@seas.upenn.edu

Albert P. Pisano
University of California

Postprint version. Published in *Sensors and Actuators A-Physical*, Volume 136, Issue 2, Special Issue SI, May 2007, pages 638-645.

Two-Port Stacked Piezoelectric Aluminum Nitride Contour-Mode Resonant MEMS

Abstract
This paper reports on design, fabrication and experimental testing of a new class of two-port stacked piezoelectric aluminum nitride contour-mode micromechanical resonators that can be used for RF filtering and timing applications. This novel design consists of two layers of thin film AlN stacked on top of each other and excited in contour mode shapes using the d_{31} piezoelectric coefficient. Main feature of this design is the ability to reduce capacitive parasitic feedthrough between input and output signals while maintaining strong electromechanical coupling. For example, these piezoelectric contour-mode resonators show a quality factor of 1,700 in air and a motional resistances as low as 175 Ω at a frequency of 82.8 MHz. The input to output capacitance has been limited to values below 80 fF, therefore simplifying signal detection even at high frequencies.

Keywords
piezoelectric resonators, two-port resonators, RF MEMS, contour-mode, aluminum, nitride

Comments
Postprint version. Published in *Sensors and Actuators A-Physical*, Volume 136, Issue 2, Special Issue SI, May 2007, pages 638-645.

Two-Port Stacked Piezoelectric Aluminum Nitride Contour-Mode Resonant MEMS

Gianluca Piazza[1] and Albert P. Pisano[2]
[1]Department of Electrical and Systems Engineering, University of Pennsylvania, Philadelphia, PA, 19104
[2]Berkeley Sensor and Actuator Center, University of California Berkeley, Berkeley, CA, 94720

Abstract

This paper reports on design, fabrication and experimental testing of a new class of two-port stacked piezoelectric aluminum nitride contour-mode micromechanical resonators that can be used for RF filtering and timing applications. This novel design consists of two layers of thin film AlN stacked on top of each other and excited in contour mode shapes using the d_{31} piezoelectric coefficient. Main feature of this design is the ability to reduce capacitive parasitic feedthrough between input and output signals while maintaining strong electromechanical coupling. For example, these piezoelectric contour-mode resonators show a quality factor of 1,700 in air and a motional resistances as low as 175 Ω at a frequency of 82.8 MHz. The input to output capacitance has been limited to values below 80 fF, therefore simplifying signal detection even at high frequencies.

Keywords: Piezoelectric resonators, two-port resonators, RF MEMS, contour-mode, aluminum nitride.

Introduction

Next-generation RF communications links will require integrated, miniaturized and microfabricated vibrating microstructures that will perform time keeping and filtering functions, consume little power and be able to span multiple frequencies on the same chip. Recent research results have demonstrated high-Q, electrostatically actuated resonators [1-4]. Although very

promising, these devices suffer from a large motional resistance, which makes their interface with 50 Ω systems very difficult. Recent efforts trying to lower the motional resistance by acting on geometrical parameters [5, 6] have not shown very significant improvements. The use of an internal electrostatic transduction mechanism [7-9] (a high-K dielectric is used to produce electrostatic forces) is very promising, but is limited by the intrinsically large capacitance that make signal detection extremely complicated at high frequencies.

Piezoelectric resonators such as thin film bulk acoustic resonators (FBARs) [10, 11] and quartz shear resonators [12] have demonstrated high quality factors and low motional resistance (few Ωs) even at GHz frequencies. Despite being proven technologies, FBARs and shear-mode quartz resonators do not permit the manufacturing of a single-chip RF module, because multiple frequency selective arrays of piezoelectric resonators cannot be fabricated on the same substrate, since film thickness sets frequency.

AlN contour-mode resonators, recently introduced by the same authors [13-15], have instead demonstrated the ability to provide multiple frequency of operation on the same substrate in combination with low motional resistance (50-700 Ω) and high quality factors (up to 4,300). At high frequencies (GHz range), these piezoelectric microstructures seem to be primarily limited by capacitive feedthrough. The resonator signal is masked by a parallel parasitic capacitance due to the fabrication process and the use of one-port configurations. In this work, a new class of contour-mode piezoelectric resonators that eliminates this feedthrough problem is introduced. This novel design consists of two AlN contour-mode microresonators stacked on top of each other and having a common ground electrode in the middle of the structure. Each resonator can be employed either as an actuation or sensing element. By physically separating the input from the output, true two-port micromechanical resonators (or resonant transformers)

have been fabricated. The only feedthrough capacitance that can ultimately limit the high frequency performance of these microdevices derives from the substrate or the AlN film itself. These resonators, in the shape of either rectangular plates or circular rings, have initially been demonstrated at frequencies as high as 214.5 MHz with a quality factor, Q, of approximately 1,500 in ambient conditions and a motional resistance, R_M, as low as 150 Ω. The feedthrough capacitance was always limited to less than 80 fF. These devices resolve the feedthrough problem encountered with one-port devices and have the potential to be extended to GHz frequencies.

In addition this novel topology can be employed to implement single-ended to differential microstructures that can reduce the number of components count by eliminating, for example, baluns. It is also possible to envision the use of these two-port stacked resonant microstructures for the implementation of mixing functions by using the non-linear actuation principle typical of "internal electrostatic" transduction that can be obtained from very thin dielectric layers [7-9].

Design of Two-Port Stacked Resonators

Figure 1 shows a possible embodiment of a two-port stacked contour-mode AlN piezoelectric resonator. This rectangular plate is formed by two c-axis oriented aluminum nitride layers, each sandwiched between two electrodes (platinum or aluminum) and vibrates in a contour mode shape. A similar stacked topology can also be realized in circular ring structures. A vertical electric field is applied to one of the two layers and induces in plane dilation of the plate through the d_{31} piezoelectric coefficient. The rectangular plate can be excited into two fundamental modes, either a length-extensional (Figure 1b) or a width-extensional (Figure 1c) mode, being the center frequency set either by the width or length of the plate, respectively. Although lower frequency flexural modes could be excited in this structure (bending can be

induced by the non-symmetric application of the input force), these mode shapes are generally characterized by larger motional resistance and very small quality factor in air and therefore go undetected (as proven by the experimental results). In a similar manner the circular ring can be excited in a radial-extensional mode of vibration, whose fundamental frequency is determined by the width of the annulus (Figure 2). At resonance, the large strain induced in the plate produces a charge that can be piezoelectrically sensed by the other layer. This vertical two port topology permits the physical separation of the input electrode from the output electrode, therefore reducing parasitic feedthrough. This two port implementation differs from the one reported by the same authors in [16] (Figure 3), because the whole top surface of the plate is now covered by one electrode and maximum electromechanical coupling is achieved [17, 18]. By moving from a horizontal two-port configuration to a vertical two-port topology, the direct feedthrough that is experienced through the device in [16] and that would have been extremely problematic at very high frequencies is eliminated (Figure 3). For the same geometry reported in [16] (200x50 μm) the feedthrough level was reduced from -40 dB to – 58 dB at approximately 19 MHz, therefore obtaining approximately an 8 fold reduction in the feedthrough capacitance from 640 fF to 80 fF.

In Figure 4 is shown the equivalent electrical model of such resonant microstructure. Each layer can be modeled using the standard Mason's model [17] (Figure 4a), for which the conversion from electrical to mechanical energy, E_M, is represented by a transformer with a turn ratio equivalent to the electromechanical coupling, η. As derived in [15] the equivalent parameters of the resonator are expressed by the following equations (these values are for the length-extensional mode, but apply to the width-extensional mode if L is substituted by W and vice versa) :

$$C_O \approx \varepsilon_o \varepsilon_{33} \frac{WL}{T} \qquad R_m = \frac{\pi}{8} TW \frac{\sqrt{E_{eq}\rho_{eq}}}{Q} \qquad L_m = \frac{\rho_{eq} LWT}{2}$$
$$C_m = \frac{2}{\pi^2 E_{eq}} \frac{L}{WT} \qquad \eta = 2d_{31} E_{eq} W \qquad \omega_o = \frac{\pi}{\mathrm{L}} \sqrt{\frac{E_{eq}}{\rho_{eq}}} \tag{1}$$

where ε_o and ε_{33} are the dielectric permittivity of air and the relative permittivity of AlN in the 3 direction (c-axis); W, L and T refers to the geometrical dimensions of the structure being respectively the width, the length and the thickness of the plate; E_{eq} and ρ_{eq} are the equivalent in-plane modulus of elasticity and mass density of AlN and the stacked electrodes and ω_o is the natural frequency of the resonator. Similar equations apply for the circular ring and are given by:

$$C_O \approx \varepsilon_o \varepsilon_{33} \frac{2\pi R_{AVE} W}{T} \qquad R_m \approx \frac{\pi}{8} 2\pi R_{AVE} T \frac{\sqrt{E_{eq}\rho_{eq}\left(1-\sigma^2\right)}}{Q} \qquad L_m \approx \frac{\rho_{eq} 2\pi R_{AVE} WT}{2}$$
$$C_m \approx \frac{2}{\pi^2} \frac{1}{E_{eq}\left(1-\sigma^2\right)} \frac{W}{2\pi R_{AVE} T} \qquad \eta = 2d_{31} E_{eq} \pi R_{AVE} \qquad \omega_o \approx \frac{\pi}{W} \sqrt{\frac{E_{eq}}{\rho_{eq}(1-\sigma^2)}}$$

(2)

where the variables are the same that were defined for equation (1), R_{AVE} is the average radius of the ring and σ is the in-plane equivalent Poisson's ratio for AlN.

The overall model describing the two-port stacked system can be obtained by combining two Mason's models together, using one for the actuation element and one for the sensing element and assuming that the two are exchanging the same electromechanical energy. As shown in Figure 4, the overall microsystem can be described by a transformer, a single resonator in the series branch and two physical parallel capacitors. The equivalent parameters of the two-stacked system can be expressed as:

$$C_{in} \approx \varepsilon_o \varepsilon_{33} \frac{WL}{T_1} \qquad C_{out} \approx \varepsilon_o \varepsilon_{33} \frac{WL}{T_2}$$

$$R_M = \frac{\pi}{8}(T_1 + T_2) W \frac{\sqrt{E_{eq}\rho_{eq}}}{\eta_1^2 Q} \quad C_M = \frac{2\eta_1^2}{\pi^2 E_{eq}} \frac{L}{W(T_1 + T_2)} \tag{3}$$

$$L_M = \frac{\rho_{eq} LW(T_1 + T_2)}{2\eta_1^2} \qquad N = \frac{\eta_1}{\eta_2}$$

where the subscript 1 and 2 refers to the actuation and sensing elements, respectively. This description represents the most general case; in this particular work η_1 and η_2 are designed to be the same and N is equal to one. The feedthrough capacitor, C_{ft}, that is included in the model (Figure 4) takes into account parasitic capacitances through the substrate, the AlN film and air. This capacitor differs from the one in [16] because it is not due to the device itself and therefore takes on a much lower value. Similar equations can also be derived for the equivalent electrical parameters of the ring structure.

It is also important to note that in this configuration the current flows in different direction in the actuation and sensing elements, as indicated by the dots in the transformer. This feature permits to avoid Q loading induced by the electrical resistance in the ground electrode. The currents are flowing in and out of the ground electrode, creating a virtual ground at this location (Figure 5). Ideally, a thin Pt electrode (< 50 nm) can be chosen for the ground electrode. Different thicknesses can be selected for the two stacked layers. A symmetric configuration, with the same thickness for both layers, can reduce the out-of-plane motion of the structure and improve isolation between input and output. The use of a thin layer might instead enable new applications, such as mixing, induced by "internal electrostatic" actuation [7-9]. Fabrication issues also set limitations in the choice of the layer thickness. In the fabrication section it will be shown that films deposited on a very thin seed layer generally show larger value of the full width half maximum (FWHM) angle that is obtained from rocking curve

measurements. FWHM values are a measure inversely proportional to the degree of crystallinity of the film and consequently of its quality. Two main configurations have been analyzed experimentally: a non-symmetric topology in which a 1.95 μm thick layer is deposited on top of a 150 nm thick AlN film and a symmetric structure with two stacked layers having the same thickness of 1 μm. For the ring structure, just the second type of implementation was tested experimentally.

Fabrication Process

Figure 6 schematically represents the simple process flow that was employed for the fabrication of these microstructures. The steps are substantially the same that were presented in [14], except for the patterning of the intermediate Pt electrode. For the intermediate Pt electrode, a lift off process was performed with the attention to use an ion-free developer that would not attack the AlN film. All the steps involved in the fabrication process occur at low temperature (T_{max} < 400 °C), therefore making these microdevices potentially post-CMOS compatible. Also, this two-layer structure requires two subsequent depositions of AlN films. Highly polycrystalline AlN piezoelectric films are sputter-deposited using an AMS single module tool and show very good rocking curve values of approximately 1.3°. It is worth reporting that the overall quality of the stack is slightly degraded when the second layer is deposited on top of a very thin (150 nm) AlN layer; for this case the rocking curve value is approximately 2.6°. Figure 7 shows a cross sectional view of the 1μm/1μm AlN stack for which columnar growth is evident and a rocking curve value of 1.3° was obtained.

Scanning electron micrographs of the fabricated microstructures are shown in Figure 8. The rectangular plate has an aspect ratio of 4:1 (length of 200 μm and width of 50 μm). Two

implementations were used for the stacked topology. In the first one a very thin AlN layer (approximately 150 nm thick) was used and on top of it a 1.95 μm thick AlN layer was deposited. In the second one the structure was kept symmetric by making both layers approximately 1 μm thick. The two AlN layers are stacked on top of each other and sandwiched between two electrodes. In the first configuration the Pt electrodes are both 100 nm thick, whereas the top Al electrode is 150 nm thick; in the second configuration the bottom electrode is 220 nm thick, whereas the ground is only 40 nm thick; the same thickness is used for the top Al electrode. A very thin electrode layer was used for the ground in the second configuration to prove that electrical loading in the ground electrode is negligible for this two port configuration. A 40 nm thick ground platinum electrode is in fact responsible for approximately 20-30 Ω of resistance in the rectangular plate configuration and would significantly load the resonator Q when excited in the width extensional mode. The circular ring has an average radius of 100 μm, a width of 20 μm and is formed by two stacked AlN layers, each having a thickness of 1 μm. In order to improve the structural symmetry of the ring, 220 nm thick Pt electrodes were used for the top and bottom electrode, whereas a thin 40 nm Pt layer was employed for the ground electrode. In order to minimize the anchors' interference with the fundamental radial-extensional mode shape, the ring structure (as shown in Figure 8) was anchored at a single location requiring routing the output signal in close proximity of the input signal. Although in this case the feedthrough capacitance was limited to 70 fF, this routing selection could ultimately limit the effectiveness of the isolation induced by the two port solution.

Experimental Results

Two-port contour-mode resonators were tested in an RF probe station at ambient pressure, using ground-signal-ground (GSG) probes. Standard Short Open Load and Through

(SOLT) calibration was performed on a ceramic substrate from Picoprobe. The microfabricated rectangular plate (Figure 8) can be excited in both length-extensional and width-extensional mode shapes. Both solutions with different layer thicknesses (from here on the 150 nm/1.95 μm stack is named solution 1 and the 1 μm/1 μm stack is named solution 2) were analyzed.

The typical electrical response of a rectangular plate resonator excited in a length extensional mode and implementing solution 2 is shown in Figure 9. The resonator shows relatively high quality factor of 2,600 in air at 19.31 MHz and a motional resistance of approximately 650 Ω. An even lower motional resistance of 175 Ω is recorded for the same resonator excited in the width extensional mode (Figure 10). Despite the lower quality factor (1,700), the resonator has a larger electromechanical coupling because it is now effectively using the length of the plate for actuation and therefore achieves a lower motional resistance.

Fundamental results for both implementations are summarized in Table I. Both solutions exhibited similar quality factors, Q, in both mode shapes, showing that the Q is probably limited by the mechanical structure and electrodes material. Also, the use of a thin electrode for the ground electrode in configuration 2 proves that a virtual ground was established and no electrical loading is experienced in this two-port configuration.

Lower motional resistance is recorded for the resonators in solution 2 and it is probably due to a larger piezoelectric coefficient than the one exhibited by the 150 nm thick element. It is believed that the very thin layer does not have the same piezoelectric coefficient of the thicker counterparts as it is also attested by the higher overall rocking curve value reported for stacked films in solution 1 (2.6° for solution 1 vs. 1.3° for solution 2).

Figure 10 compares the experimental results for a 200 x 50 μm rectangular plate excited in a width-extensional mode shape with the theoretical predictions based on the model shown in

the design section. The Q of the resonator was taken from the experimental results (a method to theoretically derive the Q factor of the resonator has not yet been devised) and a 20 fF capacitance between the input and output stages was included in the model to improve the agreement between theory and practice. This capacitance models the feedthrough introduced by the substrate, the AlN film and air. As shown by the two traces in Figure 10, there is a relatively close agreement between the predicted resonator performance and the experimental data. The equivalent mechanical properties (Young's modulus and density) of the resonator stack were computed by taking into account the mass loading effect due to Pt as discussed in [15, 19].

The circular ring response (Figure 11) is not as clean as the one of the rectangular plate and spurious modes tend to overlap with the fundamental mode. The resonator still has an unloaded Q of 1,500 and an R_M of 150 Ω at 214.5 MHz. In this case, the feedthrough capacitance is in the order of 70 fF. This is due to the proximity of input and output electrodes that are routed through the same anchor. The S_{21} plots for both the rectangular plate and circular ring apparently show responses that can be generated by pure LCR circuits (without a parallel or feedthrough capacitance) or devices with large electromechanical coupling coefficient, k_t^2 (from plot k_t^2 is larger than 8%) if the coupling is computed directly from the plot as $\frac{\pi^2}{4}\frac{f_P - f_S}{f_S}$ (where f_P and f_S correspond to the parallel and series resonant frequency, respectively). This is just an artifact of the measurement method in which the large input and output capacitances (approximately 1.6 pF for the rectangular plate) are shunted and masked by the 50 Ω termination resistors of the network analyzer. The overall model presented in the design section should instead apply, and the input and output capacitances need to be taken into account, especially when the resonators are arranged in filter arrays or placed in oscillator circuits. The electromechanical coupling for these devices should be correctly computed as the ratio of the

motional capacitance to the static capacitance of the device ($k_t^2 = \frac{\pi^2}{8}\frac{C_m}{C_{out}}$) and it is approximately 0.41%. Although the two port implementation does not improve the effective electromechanical coupling, nonetheless it does offer the capability of reducing electrical feedthrough between input and output ports.

The same resonator can be operated as a resonant transformer. As shown in Figure 12, voltage gain of approximately 4 can be obtained with a rectangular plate vibrating in the width-extensional mode at approximately 83 MHz. The curve shown in Figure 12 is simulated and it is based on the S-parameter extracted from direct measurements of the device. The resonant transformer is driving a purely resistive load of 100 kΩ. In general, most of the loads driven by resonant transformers have a capacitive component in parallel with the resistive element. This particular transformer is limited to drive a max capacitance value of 4 pF, beyond which the voltage gain is reduced to less than 1. Although interesting from an academic point of view, the use of this transformer for practical applications is limited by the power handling of the device which cannot exceed few mW.

Conclusions

For the first time, two-port stacked contour-mode AlN piezoelectric micromechanical resonators have been presented. These resonators were designed with the precise intent of reducing parasitic feedthrough between the input and the output stages of the device by physically separating the two locations. As shown by the experimental results, the feedthrough capacitance was reduced to few 10s fF, while high electromechanical coupling was maintained. At the same time, high Q factors and low motional resistance even in ambient conditions were demonstrated, showing the possibility to use these microsystems for time keeping and filtering

functions. The reduction in feedthrough capacitance makes possible the measurement of resonators at higher frequencies (GHz), previously impossible because of the large feedthrough capacitance that masked the resonator response. Therefore the authors believe that this new design will enable the contour-mode piezoelectric technology to reach GHz frequencies.

Acknowledgements

This work was supported by CSAC DARPA grant No. NBCH1020005. The authors wish to thank AMS Inc. for equipment support, the Berkeley microfabrication facility staff for their help and Philip J. Stephanou for helpful discussions.

References

[1] L. Sheng-Shian, L. Yu-Wei, X. Yuan, R. Zeying, and C.-C. Nguyen, "Micromechanical "hollow-disk" ring resonators," *17th IEEE International Conference on Micro Electro Mechanical Systems, MEMS 2004,* pp.821-4, 2004.

[2] S. A. Bhave, G. Di, R. Maboudian, and R. T. Howe, "Fully-differential poly-SiC Lame mode resonator and checkerboard filter," *18th IEEE International Conference on Micro Electro Mechanical Systems, MEMS 2005,* pp.223-6, 2005.

[3] S. Pourkamali, G. K. Ho, and F. Ayazi, "Vertical capacitive SiBARs," *18th IEEE International Conference on Micro Electro Mechanical Systems, MEMS 2005,* pp.211-14, 2005.

[4] W. Jing, J. E. Butler, T. Feygelson, and C.-C. Nguyen, "1.51-GHz nanocrystalline diamond micromechanical disk resonator with material-mismatched isolating support," *17th IEEE International Conference on Micro Electro Mechanical Systems, MEMS 2004,* pp.641-4, 2004.

[5] B. Bircumshaw, G. Liu, H. Takeuchi, K. Tsu-Jae, R. Howe, O. O'Reilly, and A. Pisano, "The radial bulk annular resonator: towards a 50 Omega RF MEMS filter," *12th International Conference on Solid-State Sensors, Actuators and Microsystems, TRANSDUCERS '03,* pp.875-8 vol.1, 2003.

[6] S. Pourkamali and F. Ayazi, "High frequency capacitive micromechanical resonators with reduced motional resistance using the HARPSS technology," *2004 Topical Meeting on Silicon Monolithic Integrated Circuits in RF Systems,* pp.147-50, 2004.

[7] S. A. Bhave and R. T. Howe, "Internal Electrostatic Transduction for Bulk MEMS Resonators," *2004 Solid State Sensor, Actuator and Microsystems Workshop*, *Hilton Head 2004,* pp. 59-60, 2004.

[8] S. A. Bhave and R. T. Howe, "Silicon nitride-on-silicon bar resonator using internal electrostatic transduction," *Solid-State Sensors, Actuators and Microsystems, TRANSDUCERS '05,* pp. 2139 - 2142, 2005.

[9] Chandrahalim H., Weinstein D., Cheow L.F., and S. A. Bhave, "Channel-Select Micromechanical Filters Using High-K Dielectrically Transduced MEMS Resonators," *19th IEEE International Conference on Micro Electro Mechanical Systems MEMS 2006*, pp. 894-897, 2006.

[10] K. M. Lakin, "A review of thin-film resonator technology," *IEEE Microwave Magazine*, vol. 4, pp. 61-7, 2003.

[11] R. Ruby, P. Bradley, J. D. Larson, III, and Y. Oshmyansky, "PCS 1900 MHz duplexer using thin film bulk acoustic resonators (FBARs)," *Electronics Letters*, vol. 35, pp. 794-5, 1999.

[12] D. T. Chang, F. P. Stratton, D. J. Kirby, R. J. Joyce, T.-Y. Hsu, and R. L. Kubena, "A New MEMS-Based Quartz Resonator Technology," *Solid State Sensor, Actuator and Microsystems Workshop*, *Hilton Head 2004,* pp. 41-44, 2004.

[13] G. Piazza, P. J. Stephanou, J. M. Porter, M. B. J. Wijesundara, and A. P. Pisano, "Low motional resistance ring-shaped contour-mode aluminum nitride piezoelectric micromechanical resonators for UHF applications," *18th IEEE International Conference on Micro Electro Mechanical Systems, MEMS 2005,* pp.20-3, 2005.

[14] G. Piazza, P. J. Stephanou, M. B. J. Wijesundara, and A. P. Pisano, "Single-chip multiple-frequency filters based on contour-mode aluminum nitride piezoelectric micromechanical resonators," *Solid-State Sensors, Actuators and Microsystems, 2005, TRANSDUCERS '05,* pp. 2065-2068, 2005.

[15] G. Piazza, "Piezoelectric Aluminum Nitride Vibrating RF MEMS for Radio Front-End Technology," Ph.D. Thesis in Electrical Engineering and Computer Science, University of California Berkeley, 2005.

[16] G. Piazza and A. P. Pisano, "Dry-Released Post-CMOS Compatible Contour-Mode Aluminum Nitride Micromechanical Resonators for VHF Applications," *2004 Solid-State Sensor, Actuator and Microsystems Workshop, Hilton Head 2004,* pp. 37-40, 2004.

[17] J. F. Rosenbaum, *Bulk Acoustic Wave Theory and Devices*, Artech House, Inc., 1988.

[18] W. G. Cady, *Piezoelectricity; an introduction to the theory and applications of electromechanical phenomena in crystals*. New York, London: McGraw-Hill Book Company, Inc., 1946.

[19] P. J. Stephanou, G. Piazza, C. D. White, M. B. J. Wijesundara, and A. P. Pisano, "Piezoelectric Thin Film AlN Annular Dual Contour Mode Bandpass Filter," *Proceedings of ASME IMECE 2005*, 2005.

List of Figures and Tables

values of the Young's modulus, $E_{eq,}$ and density, ρ_{eq}, for the stacked resonator take into account the loading due to the electrode materials as specified in [19].

Figure 11: *S_{21} response for a two-port stacked circular ring resonator having a width of 20 μm and average radius of 100 μm. Despite the spurious modes, the response shows limited capacitive feedthrough (70 fF) between input and output.*

Figure 12: *Experimental data for a 200 x 50 μm rectangular plate vibrating in the width-extensional mode and operated as a transformer. The 100 kΩ load is simulated and the device performance was derived from the scattering parameters of the device. It should be noted that the maximum capacitive load that can be drive in parallel with the resistive load is 4 pF. Capacitances beyond 4 pF can degrade the performance of the resonant transformer and reduce its gain below 1.*

Biography

Gianluca Piazza is an Assistant Professor in the department of Electrical and Systems Engineering (ESE) at the University of Pennsylvania. His research interests focus on piezoelectric micro and nano systems (MEMS/NEMS) for RF wireless communications, bio/chemical detection, wireless sensor platforms and medical ultrasounds. He also has general interest in the areas of micro/nano fabrication techniques and integration of micro/nano devices with state-of-the-art electronics. He received his Ph.D. degree from the University of California, Berkeley in Fall 2005, where he developed a new class of AlN contour-mode vibrating microstructures for RF communications. He has more than 6 years of experience working with piezoelectric materials, holds two patents in the field of micromechanical resonators and co-founded a start up (Harmonic Devices, Inc.) for the commercialization of piezoelectric resonators. He is a member of IEEE.

Albert ("Al") P. Pisano currently serves as Professor and Chair of the Department of Mechanical Engineering at the University of California at Berkeley. He was elected to the National Academy of Engineering in 2001. At UCB, Professor Pisano holds the FANUC Chair of Mechanical Systems in the Department of Mechanical Engineering, with a joint appointment to the Department of Electrical Engineering and Computer Science. He currently serves as a Director of the Berkeley Sensor & Actuator Center (BSAC). Professor Pisano received his B.S., M.S. and Ph.D. (1981) degrees from Columbia University in the City of New York in Mechanical Engineering. Prior to joining the faculty at UC Berkeley, he held research positions with Xerox Palo Alto Research Center, Singer Sewing Machines Corporate R&D Center, and General Motors Research Labs. From 1997-1999, he served as Program Manager for the MEMS program at the Defense Advanced Research Projects Agency (DARPA). His research interests and activities at UC Berkeley include MEMS for a wide variety of applications, including RF components, power generation, drug delivery, strain sensors, biosensors and disk-drive actuators. Professor Pisano is the co-inventor listed on 20 patents in MEMS and has authored or co-authored more than 190 archival publications. He is a co-founder in start-up companies in the area of transdermal drug delivery, transvascular drug delivery, sensorized catheters, MEMS manufacturing equipment and MEMS RF devices.

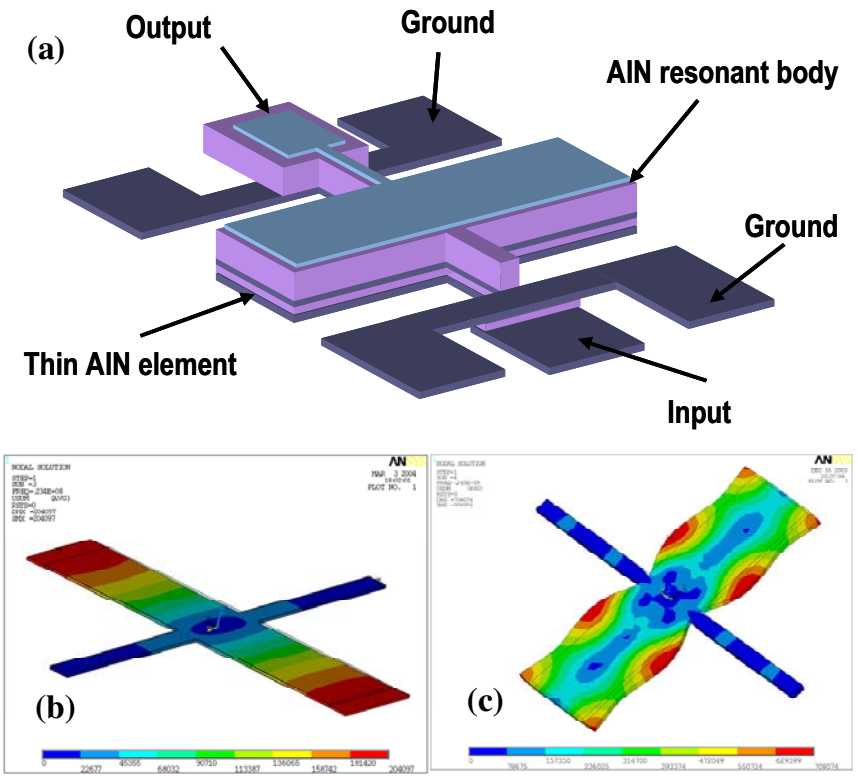

Figure 1: *(a) Schematic representation of a two-port contour-mode piezoelectric resonator; (b) ANSYS simulation for the length-extensional mode of the same resonator; (c) ANSYS simulation of the width-extensional mode shape for the same resonator.*

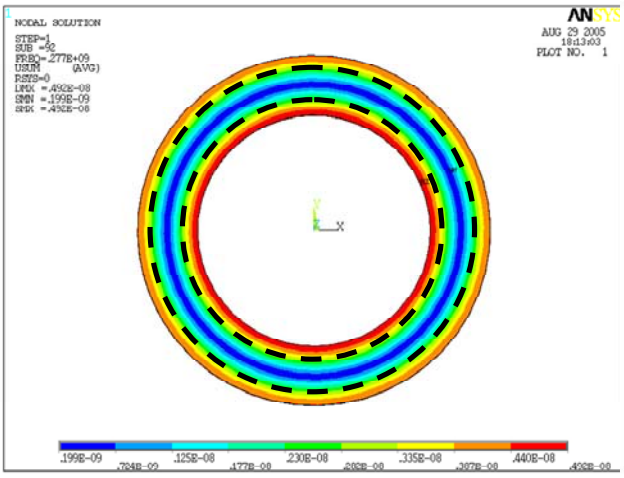

Figure 2: *ANSYS simulation of the radial-extensional mode of vibration for the circular ring structure. The width of the ring sets the resonator center frequency.*

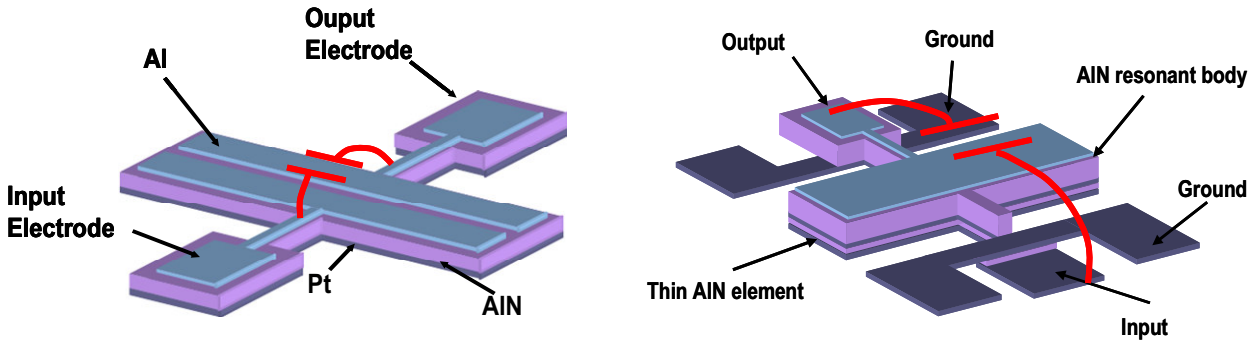

Figure 3: *Schematic representation of the reduction in parasitic feedthrough capacitance obtained by moving from a horizontal to a vertical two-port topology. The vertical stack suffers solely from substrate parasitics, whereas the horizontal structure suffers from a direct capacitance through the device.*

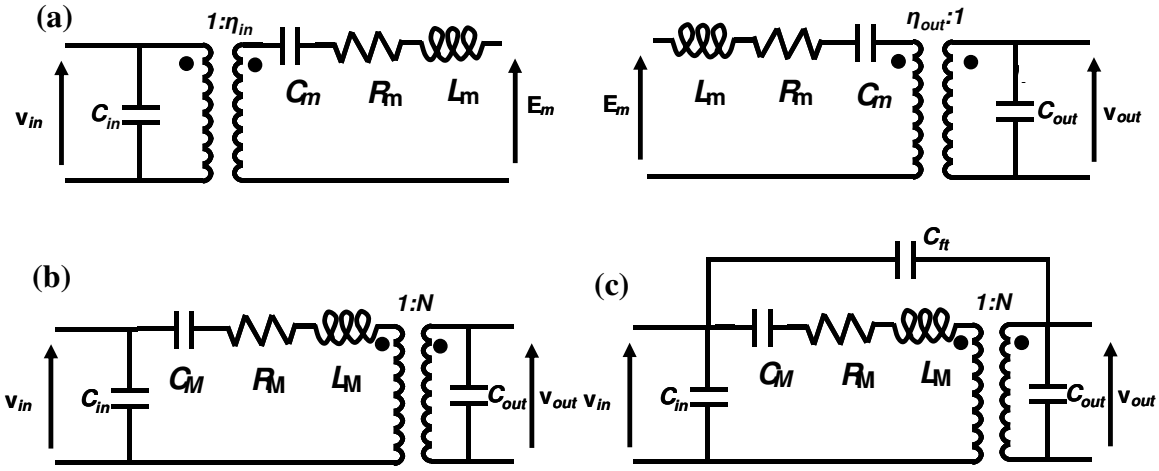

Figure 4: *Equivalent electrical model for the two-layer stacked resonator. The model includes a feedthrough capacitance due only to the substrate and possibly the AlN film. No direct feedthrough comes from the electrode layout itself. Please note the dots notation for the transformer. The current flows in different directions in the actuation and sensing elements.*

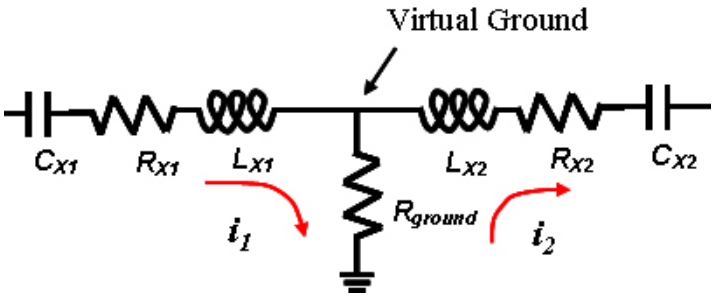

Figure 5: *Simplified equivalent electrical representation of two stacked resonators, showing that the current is flowing in opposite direction through the ground resistor, therefore realizing a virtual ground node.*

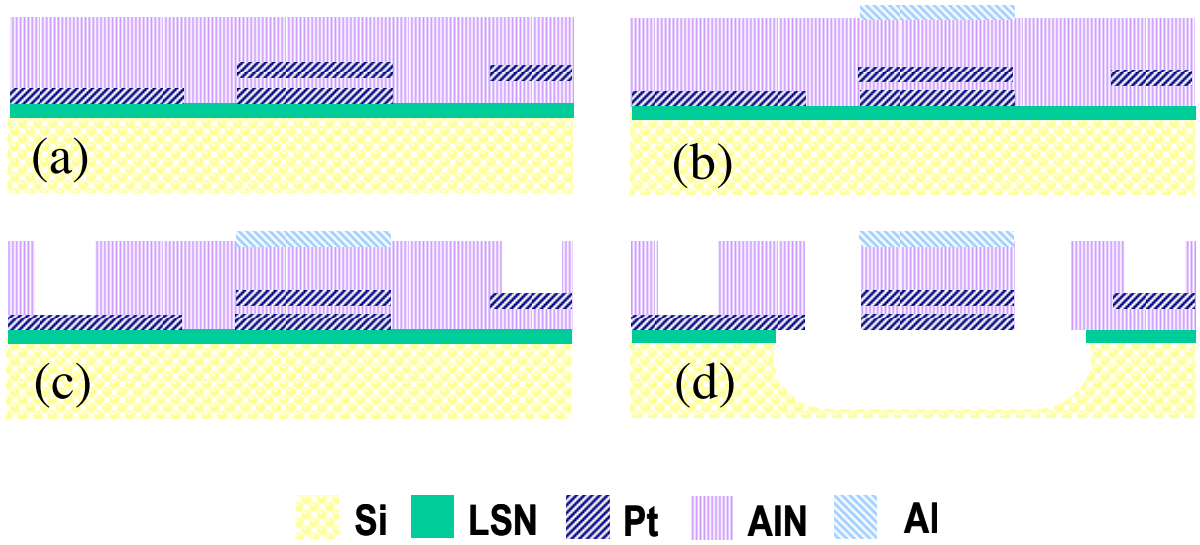

Figure 6: *Schematic representation of the process flow used to fabricate the two-port contour-mode piezoelectric resonators. (a) Low-stress nitride (LSN) is used for isolation purpose; on top of it Pt is patterned by lift off; a thin layer of AlN is sputter deposited; afterwards, the second Pt electrode is patterned by lift off and a thicker AlN layer is sputtered deposit to form the second structural layer. (b) The Al top electrode is sputter-deposited and patterned by dry etch in a Cl_2-based RIE system. (c) Contacts to the bottom and intermediate electrode are opened by wet etch of AlN in hot H_3PO_4. (d) AlN is masked by low-temperature oxide (LTO) and dry etched in a Cl_2-based RIE system. LTO and LSN are then etched and removed by dry etch. The final structure is dry released in XeF_2.*

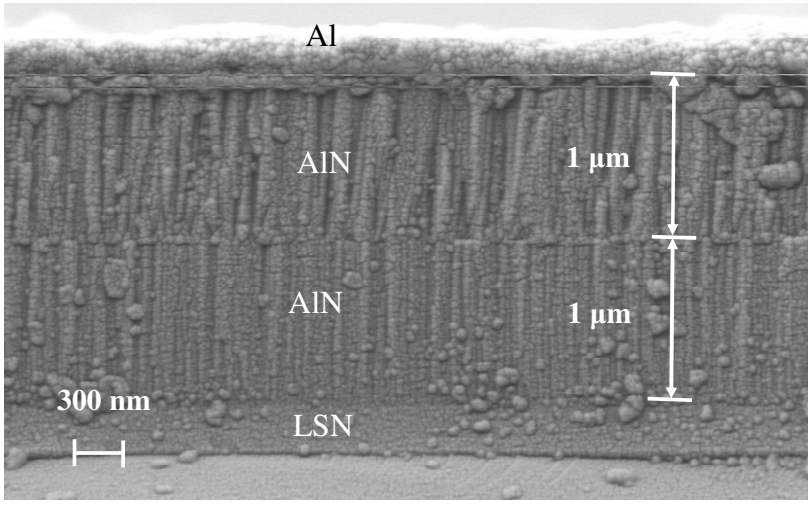

Figure 7: *Cross sectional view of two layer process. Two 1 µm AlN layers were deposited on top of each other.*

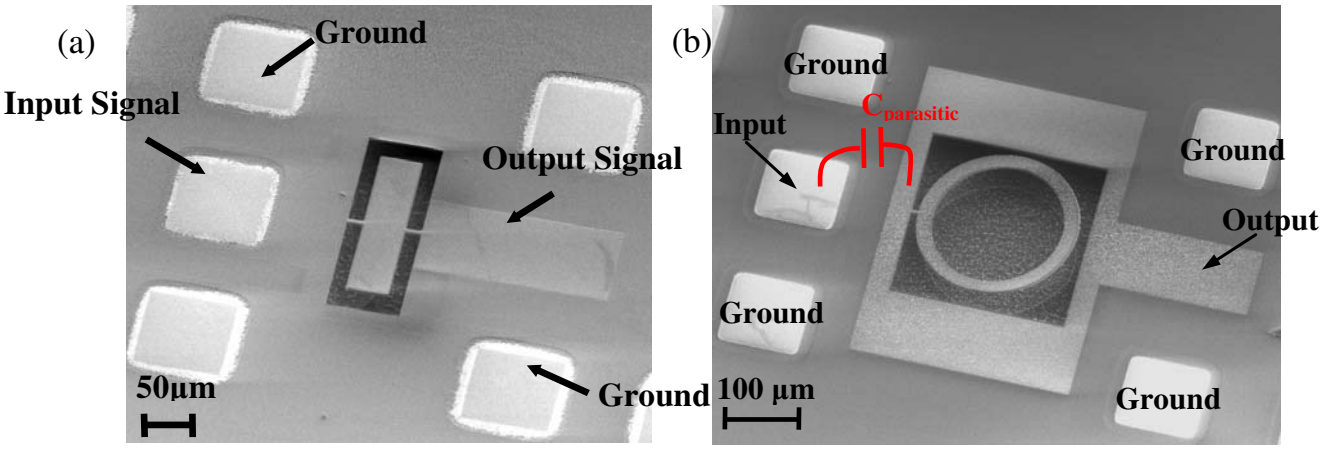

Figure 8: *Scanning electron micrographs of: (a) two-port contour-mode piezoelectric rectangular plate resonator and (b) two-port contour-mode piezoelectric ring resonators.*

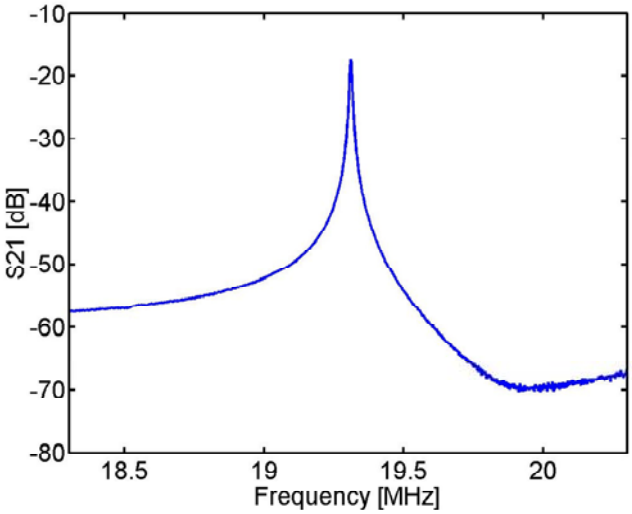

200x50 µm plate length-ext. mode
f_c=19.31 MHz
Q ~ 2,600
R_M ~650 Ω
C_{ft} ~ 80 fF

Figure 9: *Electrical response of a two-port rectangular plate piezoelectric resonator excited in the length-extensional mode shape. The stack is formed by two 1 µm thick AlN layers.*

Table I: *Summary of the experimental results obtained for two different stacked configurations. (150 nm/1.95 μm is named solution 1; 1 μm/1 μm is named solution 2). Slight differences in the feedthrough capacitance value of Sol.1 are limited by the dynamic range of the measurements and accuracy of the calibration process.*

Stack Type	**Mode**	**f_o [MHz]**	**Q**	**R_x [Ω]**	**C_f [fF]**
Sol. 1	Length-Ext.	20.24	2,300	2,900	15
	Width-Ext.	86.1	1,700	600	10
Sol. 2	Length-Ext.	19.31	2,600	650	80
	Width-Ext.	82.8	1,700	175	80

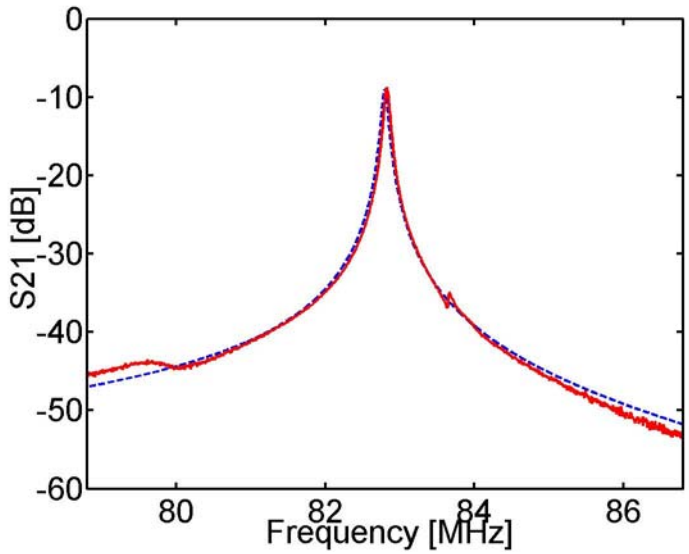

200x50 µm plate width-extensional mode shape
f_c=82.8 MHz
Q ~ 1,700
R_M ~175 Ω
C_{ft} ~ 80 fF

Resonator Variable	Width-Ext. Plate	
	THEORY	EXPERIM.
f_o [MHz]	82.82	82.82
L_M [µH]	555.6	571.8
C_M [fF]	6.65	6.46
R_M [Ω]	184	175
C_{in}, C_{out} [pF]	0.88	1.6

Parameter	Value
E_{eq}	380 GPa
ρ_{eq}	5,527 kg/m^3
d_{31}	2 pC/N
ε_{33}	10

Figure 10: *S_{21} parameters for a 200x50 µm rectangular plate excited in the width-extensional mode shape. Experimental results (continuous line) are compared with theoretical predictions (dashed line) based on the equivalent electrical model proposed in the design section. Q value was taken from the experimental results. A 80 fF feedthrough capacitance between the input and output stages was included in the theoretical model to account for the parasitics introduced by the substrate, the AlN film and air. The larger than expected value of the input and output capacitances is due to capacitive feedthrough between the routings of the input or output electrodes and the ground plane, which extend beyond the rectangular plate itself. Equivalent values of the Young's modulus, E_{eq}, and density, ρ_{eq}, for the stacked resonator take into account the loading due to the electrode materials as specified in [19].*

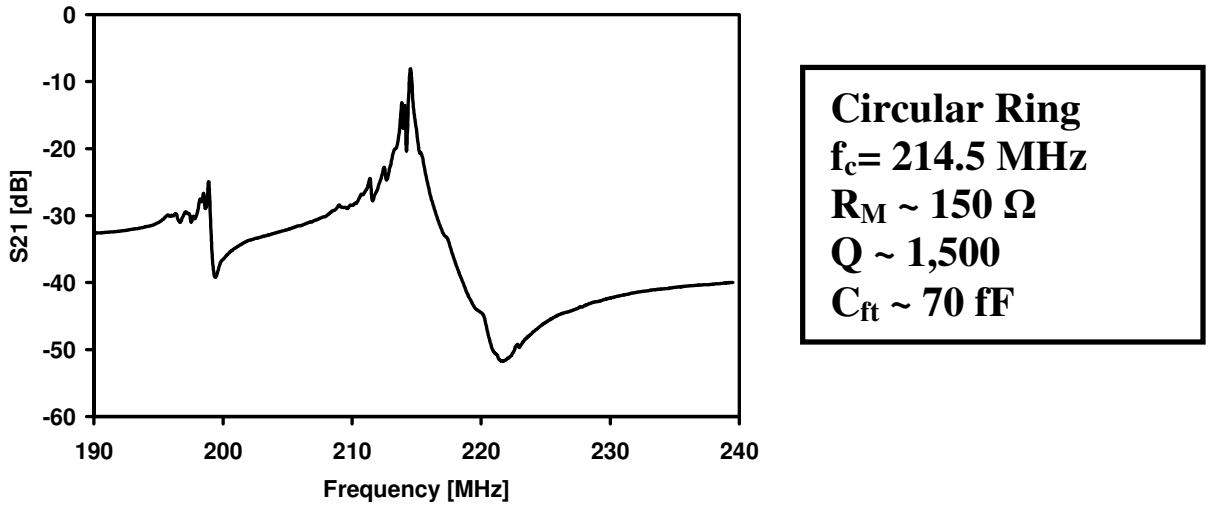

Figure 11: *S_{21} response for a two-port stacked circular ring resonator having a width of 20 μm and average radius of 100 μm. Despite the spurious modes, the response shows limited capacitive feedthrough (70 fF) between input and output.*

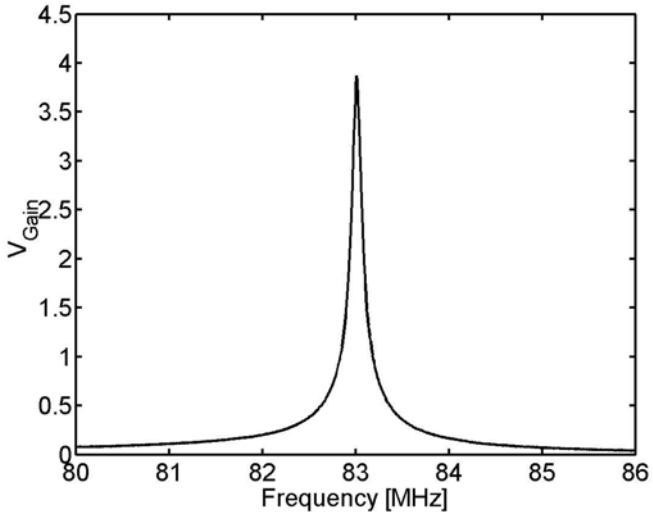

Figure 12: *Experimental data for a 200 x 50 μm rectangular plate vibrating in the width-extensional mode and operated as a transformer. The 100 kΩ load is simulated and the device performance was derived from the scattering parameters of the device. It should be noted that the maximum capacitive load that can be drive in parallel with the resistive load is 4 pF. Capacitances beyond 4 pF can degrade the performance of the resonant transformer and reduce its gain below 1.*